J Radioanal Nucl Chem (2015) 303:2313–2320
DOI 10.1007/s10967-014-3655-3

Structural effects of ZnS:Cu phosphor layers on beta radioluminescence nuclear battery

Zhi-Heng Xu · Xiao-Bin Tang · Liang Hong · Yun-Peng Liu · Da Chen

Received: 14 August 2014 / Published online: 10 October 2014

Abstract The design, fabrication, and testing of beta radioluminescence (RL) nuclear battery based on the ZnS:Cu phosphor layers with plane and V groove structures are presented. The RL spectra and current–voltage characteristic curves were used to investigate the optical and electrical properties with ^{63}Ni and ^{147}Pm. For different structures, their emission peaks are all at 530 nm. The Monte Carlo simulation code was employed to analyze the device performance. The V groove structure has the ability to provide improved for an appropriate radiation source. Overall, a suitable phosphor layer structure can provide a new route to exhibit higher energy conversion efficiency.

Keywords Beta radioluminescence nuclear battery · ZnS:Cu · Phosphor layer structure · ^{63}Ni · ^{147}Pm

Introduction

The design of electronic devices has experienced a gradual progression in the last years towards smaller scales and higher integration densities. Such is the case as microelectromechanical systems (MEMSs) [1–4]. However, the power supply remains a major challenge due to the natural conflict between the size of the system and limited power density. In this context, nuclear batteries provide a promising alternative for longer half-life and higher energy density. A typical nuclear battery offers prolonged operation times, uninterrupted energy supply, and durability in extreme environments [5]. In addition, they can be deployed in numerous fields such as portable electronics and autonomous systems, including outer space and the deep ocean. In order to realize the full potential from the nuclear batteries, an extensive research effort has been carried out to identify the determinants for energy conversion mechanisms. Beta radioluminescence (RL) nuclear batteries opened an attractive research field after radioisotope beta-voltaic batteries, due to their larger range of possible radioisotopes and feasibility of radiation protection for semiconductor materials [6]. In such power sources, a radioisotope is placed adjacent to a phosphor layer, which absorbs energetic beta particles emitted from the radioisotope source, and then re-emits the energy in the form of luminescence. The luminescence is subsequently absorbed and converted into electricity via the semiconductor materials. The indirect conversion mechanism is shown in Fig. 1. Although indirect-conversion nuclear batteries of this type shall be advantageous, their implementation is still in an early phase, with rather limited power outputs.

Extensive efforts have focused on the improvement of the energy conversion efficiency by utilizing various radiation sources and different kinds of phosphors or semiconductor materials such as single crystal silicon, GaP and AlGaAs [7–10]. However, the applications of beta RL nuclear batteries are still limited, mainly because of the low total energy conversion efficiency. For beta RL nuclear battery with a new indirect-conversion method, the phosphor layers play an important role to shield the semiconductor materials, to absorb the incident radiation, and to transport the emitted luminescence. Besides the study of energy conversion mechanisms and interactive stages, balancing the competing effects of nuclear energy absorption and luminescence transmission is a great way to

Z.-H. Xu · X.-B. Tang (✉) · L. Hong · Y.-P. Liu · D. Chen
Department of Nuclear Science and Engineering, Nanjing University of Aeronautics and Astronautics, Nanjing 211106, China
e-mail: tangxiaobin@nuaa.edu.cn

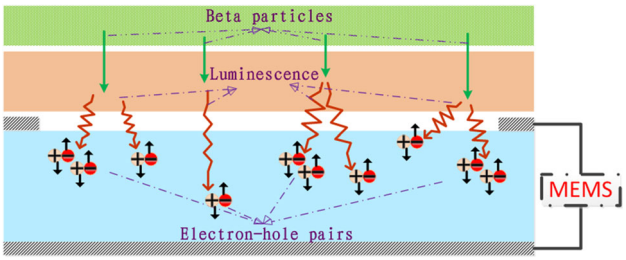

Fig. 1 Schematic of the beta RL nuclear battery

Table 1 Main properties of two beta isotopes

Isotopes	Half-life (a)	Max. energy (keV)	Ave. energy (keV)	Specific activity density (Bq/cm^2)	Date of manufacture
^{63}Ni	100.1	66.9	17.2	1.82×10^8	2011-08-11
^{147}Pm	2.6	224.6	62.1	1.07×10^8	2011-10-20

enhance the performance of batteries. In addition, the search for a proper structure of phosphor layers may offer opportunities for innovation to increase the efficiency of beta RL nuclear batteries.

The present work focused on the development of lamination-structure beta RL nuclear batteries, which were composed of InGaP/GaAs/Ge triple-junction photovoltaic (PV) devices, ZnS:Cu phosphor layers, and ^{63}Ni plate source. The feasibility of using Cu-doped ZnS as a RL phosphor under beta-particle excitation was tested. The response effects were obtained by studying the relationship between the structure of phosphor layers and the electrical characterizations. The results were compared with those obtained from the irradiation of a ^{147}Pm plate source.

Experimental

RL nuclear batteries consist of three main parts: (1) isotope emitters, (2) ZnS:Cu phosphor layers, and (3) InGaP/GaAs/Ge PV devices. First, the selection of isotope to use in a nuclear battery based on half-life, purity, energy density, and endpoint energy is critical. Penetrating radiation like gamma rays or X-rays could be used theoretically, but would require thicker shielding and large-scale nuclear battery configurations. The types of radiation sources focus on alpha and beta particles due to their relatively short ranges. Generally, within a certain radioactive decay type, the energy density varies inversely with the half-life of the isotope; the higher the power density, the shorter the half-life [6]. Considering the pursuit of a nuclear battery, long shelf life and high power density, and the characteristics of alpha sources with a high-energy-density and much more significant radiation damage, beta sources are recommended to use as the radiation source. ^{63}Ni was utilized because of its high purity of emitted beta particles with moderate energy, and its long half-life. Besides ^{63}Ni, the proposed method can use other radioisotopes with more energetic emitted beta particles, e.g. ^{147}Pm. Table 1 gives the main properties of these two beta isotopes.

ZnS:Cu is suitable for use as the phosphor layer in an indirect-conversion nuclear battery with great performance. The ZnS is an n-type A_2B_6 group intrinsic semiconductor material, which has been extensively investigated due to its potential use for various applications such as semiconductor light-emitting diode and cathode-ray displays [11]. It has a wide band gap of 3.5–3.7 eV, a high light transmittance, and a low dispersion in the visible and infrared region [12–14]. Among the conventional phosphors, ZnS:Cu is an efficient RL material with a great stability of luminescence output, and high tolerance to ionizing radiation [15]. An adhesive technique was employed to prepare ZnS:Cu phosphor layers with different structures. The phosphors were directly adhered to the transparent adhesive tape with a great viscosity and transparency. This simple and low-cost method was used to produce even and thin phosphor layers consisting of a 16 μm-thick phosphor powder and a 3 cm × 3 cm 29 μm-thick adhesion layer. A sample of a ZnS:Cu phosphor layer is shown in Fig. 2, along with a digital photograph taken under irradiation from a beta source.

In order to match the RL spectra and improve the luminescence efficiency, InGaP/GaAs/Ge triple-junction PV devices were utilized as energy conversion unit due to their wide band-gap and low leakage current. InGaP/GaAs/Ge was grown epitaxially on the Ge substrate by the metal organic chemical vapor deposition technology. Adopting the method of accumulated multiple p–n junctions can effectively increase the volume of the depletion layer and increase the energy conversion efficiency [16]. A high quality passivation window layer consisting of Al_xInP ($x = 0.5$) was introduced on the frontal surface of the devices. The passivation layer on the backside was made of an aluminum back surface field layer. The PV devices rely on this design approach to effectively improve the quantum efficiency, reduce the interface compound effect, decrease the dark current, and increase the utilization ratio of incident photon. The back electrode of the PV devices was connected with the printed circuit boards (PCBs) pad through conductive silver adhesives. The gold ball bonding technique was employed to complete the front electrode down-leads. The active area of the PV devices was 0.5 cm × 0.5 cm. In order to reduce the energy loss, the beta isotopes were directly prepared on the surface of the phosphor layer using insulated brackets to fix together the beta isotope and the PV devices, with the phosphor layer in

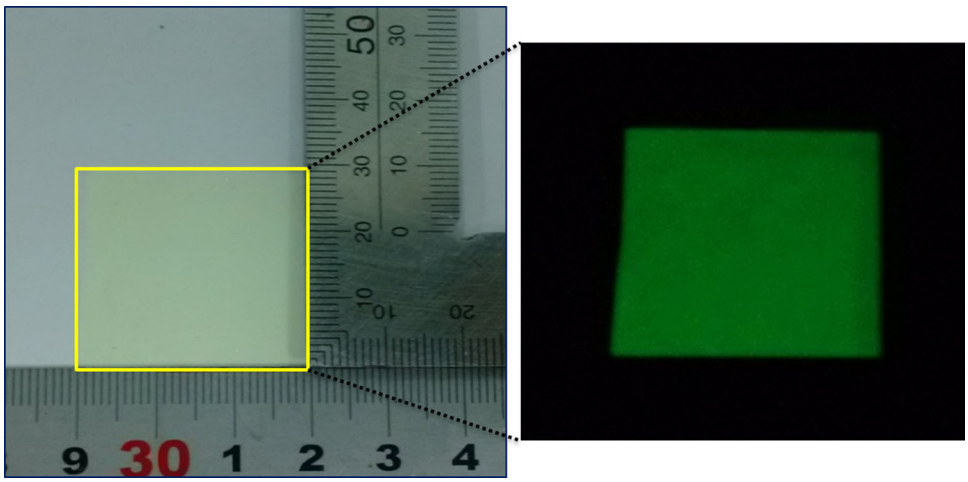

Fig. 2 Plane ZnS:Cu phosphor layer sample and RL effect

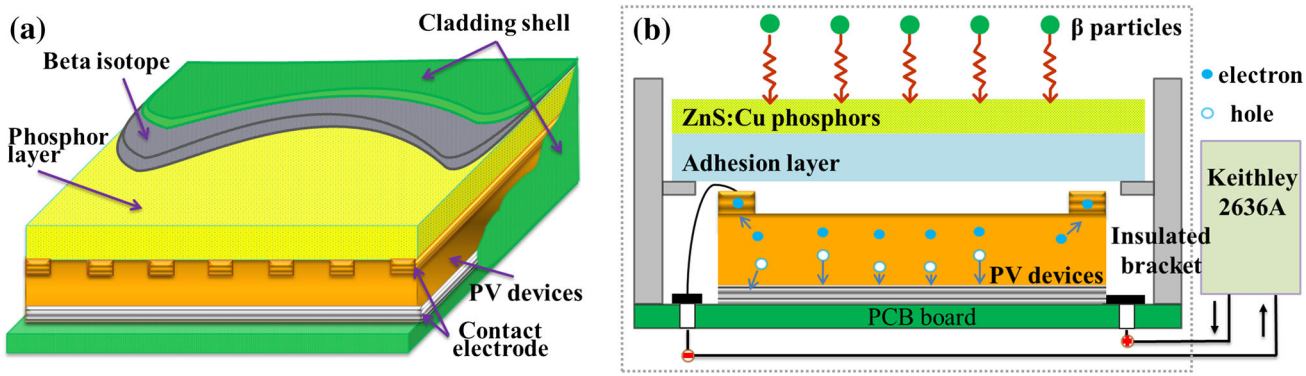

Fig. 3 The beta RL nuclear battery: **a** a three-dimensional schematic view; **b** measurement schematic graph and its energy conversion working mechanism

between. Figure 3 shows a three-dimensional schematic view of the laminated structure of the resulting beta RL nuclear battery.

The structural effects of ZnS:Cu phosphor layers on beta RL nuclear battery were tested at normal temperature and pressure values. The RL of the phosphor layers were measured by using a Cary Eclipse fluorescence spectrophotometer (Agilent Technologies, USA) with 4.93 mCi/cm^2 ^{63}Ni and 2.88 mCi/cm^2 ^{147}Pm beta-particle excitation sources. A dual-channel system source-meter instrument (Model 2636A, Keithley, USA) was used to measure the current–voltage (I–V) characteristics of the nuclear battery, which was shielded from light and electromagnetic interference under irradiation test conditions.

Results and discussion

Structure of plane phosphor layer

ZnS:Cu phosphor layers with single- and double-plane geometry are depicted in Fig. 4. In order to evaluate the performance of these two geometries, the phosphor layer was irradiation with a Φ30 mm plate ^{63}Ni source (4.56 × 10^7 Bq) and a Φ39 mm plate ^{147}Pm source (2.68 × 10^7 Bq). As shown in Fig. 5, the RL intensity strongly depends on the type of beta source used and the geometric structure of phosphor layers. On the other hand, the peak position (around 530 nm) and shape of the RL spectra have do not exhibit such dependency. Based on the high-resolution RL measurements, it is apparent that the ZnS:Cu phosphor layer was a suitable RL material, which is consistent with the previous research achievements [10, 12].

The scanning I–V curves and the outputs tested by Keithley 2636A are shown in Fig. 6 and Table 2, respectively. The latter includes the electrical performance parameters of the short-circuit current I_{sc}, the open-circuit voltage V_{oc}, and the maximum output power P_{out}. The fill factor FF can be calculated by using the following formula:

$$\mathrm{FF} = \frac{P_{out}}{I_{sc}V_{oc}} = \frac{I_m V_m}{I_{sc}V_{oc}}, \quad (1)$$

where I_m and V_m describe the bias point at which the power generation reaches a maximum. Moreover, according to the

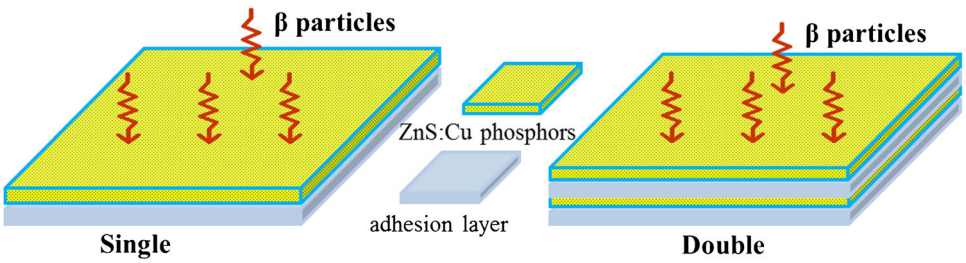

Fig. 4 The single-plane and double-plane phosphor layers

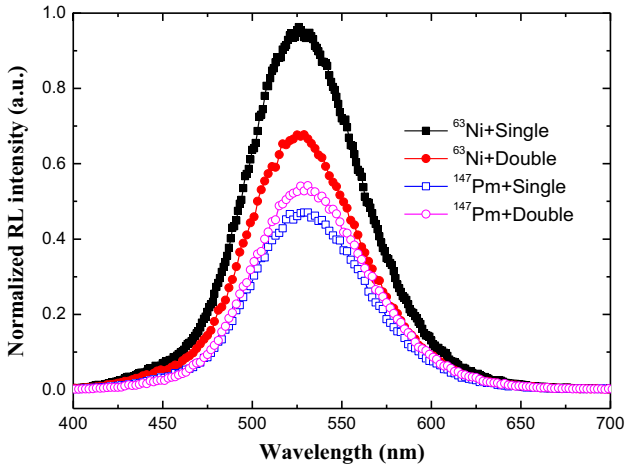

Fig. 5 RL spectra of plane phosphor layer under different beta sources

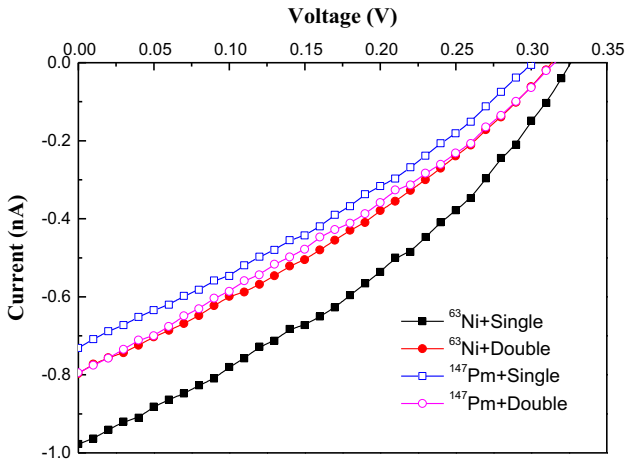

Fig. 6 I–V characteristic curves of plane phosphor layer

modified empirical formula adapted from Katz and Penfld, the beta range of ^{63}Ni and ^{147}Pm can be calculated as [17]:

$$R = 0.412E^{1.265-0.0954\ln E}/\rho, \quad E \leq 2.5\ \text{MeV}, \tag{2}$$

where R is the beta range in the phosphor layers (cm), E is the maximum energy of the beta source (MeV), and ρ is the density of the phosphors (g/cm^3). The mean ranges of beta

Table 2 The results of the nuclear battery with single- and double-plane phosphor layers

Isotopes	Structure types	V_{oc} (V)	I_{sc} (nA)	FF	P_{out} (nW)
^{63}Ni	Single-plane	0.3199	0.964	0.35	0.1075
	Double-plane	0.3099	0.776	0.32	0.0778
^{147}Pm	Single-plane	0.2999	0.709	0.32	0.0671
	Double-plane	0.3099	0.772	0.31	0.0740

particles penetrating in the ZnS:Cu phosphor layer are approximately 10.4 and 70 μm calculated respectively with the full beta spectrum of ^{63}Ni and ^{147}Pm. According to this prescription, even those particles with the maximum energy can travel 16 and 123 μm, respectively. Note that as long as the thickness of phosphor layer is thinner than the β particles penetrating range, it is possible to increase the energy deposited by the β particles by increasing the former. Since the actual thickness of the single-plane ZnS:Cu phosphor layer is close to the beta range of ^{63}Ni, so the single phosphor layer is suitable for the ^{63}Ni source, and the irradiation results show that the ^{63}Ni out-performed with V_{oc} of 0.32 V, I_{sc} of 0.96 nA and P_{max} of 0.11 nW. Even though the second phosphor layer increases the emitted luminescence, the absorption effect and the ability of blocking for the luminescence transmission will be strengthen. Consequently, when the phosphor layer structure changed from single to double, the RL intensity and the performance of the battery declined under excitation by the ^{63}Ni source. On the contrary, for the ^{147}Pm source, with a higher energy and longer range, the effects of increasing luminescence generation are stronger than blocking photon absorption. In this case, the double configuration can increase the thickness of the phosphor layer, and corresponding increase the deposited energy of beta particles or equivalently the generation of luminescence, resulting in a 10.3 % increase in the maximum output power. This is consistent with previous work in which the thickness of the phosphor layer and the efficiency of RL transmission are critical to battery design [9, 18]. Consequently, the phosphor layer should have a suitable thickness to absorb fully the incident radiation while still allowing for the transmission of luminescence [19]. Additionally, it is obvious

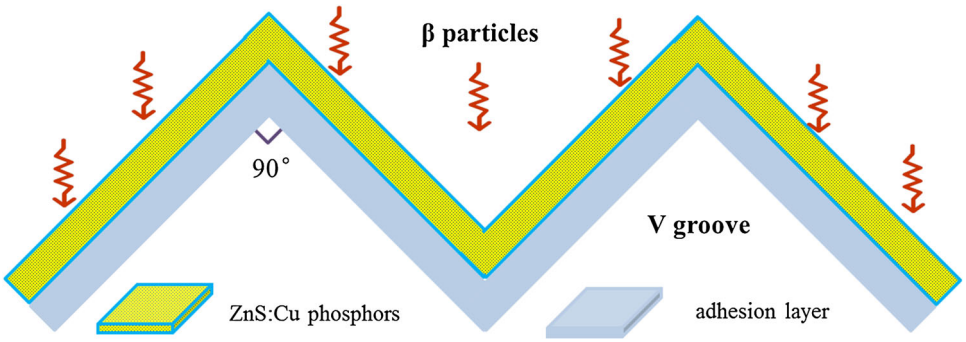

Fig. 7 The V groove phosphor layers

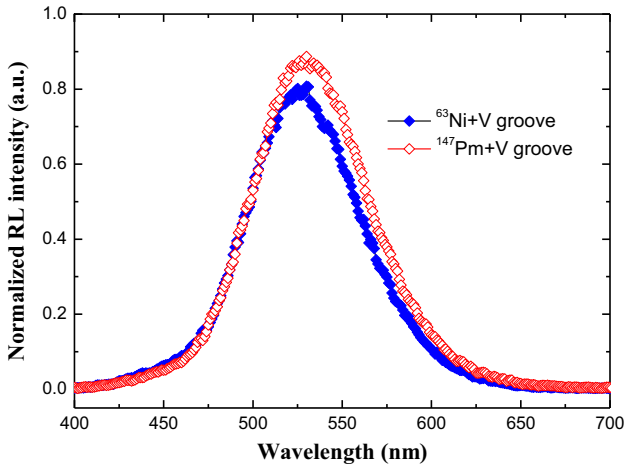

Fig. 8 RL spectra of V groove phosphor layer under different beta sources

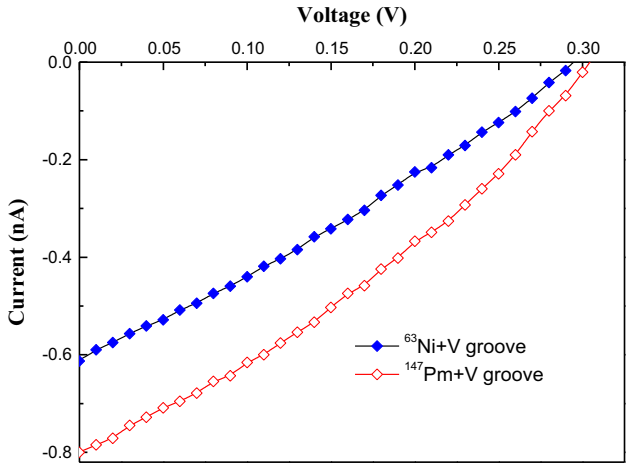

Fig. 9 I–V characteristic curves of V groove phosphor layer

that the relationship between the RL intensity and the output performances is a better positive correlation.

Structure of V groove phosphor layer

A design of V groove structure of the ZnS:Cu phosphor layer was also investigated, and the processed sample model was shown in Fig. 7. The initial size of the phosphor layers remained the same (3 cm × 3 m), while the bending angles were all 90°. Figure 8 depicts the normalized RL intensity of the ZnS:Cu phosphor layers with V groove structure. Compared with the plane structure, a reversal phenomenon was observed, namely the optical characterization of V groove phosphor layers under excitation by the ^{147}Pm was better than with the ^{63}Ni source.

The I–V characteristics curves obtained with the V groove ZnS:Cu phosphor layers irradiated by ^{63}Ni and ^{147}Pm source are shown in Fig. 9. The measured electrical performance is summarized in Table 3. From these data, it appears that the maximum output power of the "Pm–V" was higher than the "Ni–V" group, which is consistent with research in RL intensity. It is chiefly because of two opposing factors: on the one hand, the distance between the source and the PV devices in the V groove structure was longer than the plane; on the other hand, the content of the phosphor powders in unit projection area was increased for a V groove configuration. Therefore, for the RL nuclear battery with ^{63}Ni, which emit low energy β particles, the negative effect of air blocking was stronger than the positive effect of energy deposition increasing in the phosphor layer. Nevertheless, for the beta particles emitted from the ^{147}Pm source have higher energy and longer penetration depth, the V groove structure with a larger surface area can effectively increase the concentration of the phosphor powders per unit projection area, hence increasing the RL intensity. This translates into more luminescence passing through the phosphor layer to the PV devices. Thus, the maximum output power of "Pm–V" was increased 15.95 % compared to the phosphor layer with "single-plane" structure.

Theoretical calculation

Besides the experimental results discussed in the previous section, the General Monte Carlo N-Particle Transport

Table 3 The results of the nuclear battery with V groove phosphor layers

Isotopes	V_{oc} (V)	I_{sc} (nA)	FF	P_{out} (nW)
^{63}Ni	0.2899	0.590	0.30	0.0516
^{147}Pm	0.2999	0.784	0.33	0.0778

Table 4 Energy deposition percentage per unit projection area of the phosphor layers

Structure type	Single-plane	Double-plane	V groove
^{63}Ni	86.26 %	86.26 %	82.80 %
^{147}Pm	61.83 %	71.94 %	77.92 %

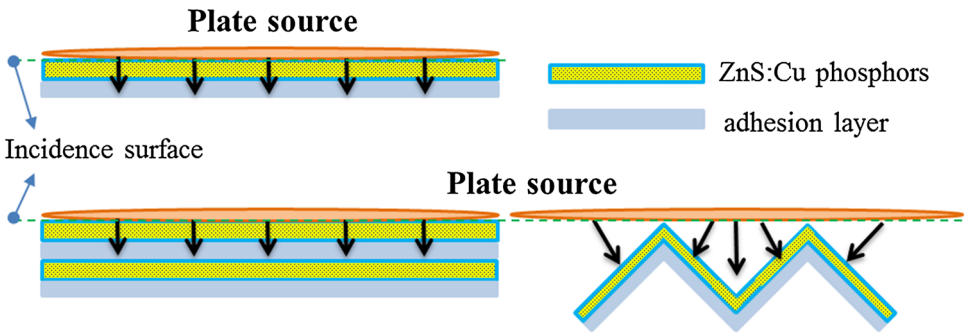

Fig. 10 The physical method for the MCNP simulation

Code Version 5 (MCNP 5) was introduced to the theoretical research, as presented in Fig. 10. To calculate the deposition energy in matter, the full beta energy spectrums were used in the model. The radius of beta plate sources was set to 1.5 cm. In the simulation of the transport process of beta particles in phosphor layers, the structure and dimension parameters were consistent with the experimental conditions.

The percentage of energy released by the beta source that was deposited into the ZnS:Cu phosphor layers was calculated. In the unit cross-sectional area of the phosphor layer projection to the PV devices surface, the results of different structures are given in Table 4. The number of simulated particles was 3×10^8, and the errors were all less than 0.05 %. For a planar geometry, the energy deposition percentage of phosphor layers were increased with the increase of laminated depth, due to the beta particle range is larger the thickness of phosphor layer. The degree of increase was different in deposition energy, though to different energy beta particles. From the results irradiated by ^{63}Ni, the research found that the second phosphor layer did little to increase the deposition energy. Furthermore, the energy deposition percentages of V groove was lower than the single-plane structure, even though they are all a single layer. However, energy deposition was increased significantly with the depth of phosphor layers increasing for the ^{147}Pm source. Meanwhile, the V groove structure was greater compared to the single-plane, which increased by almost 26 %. In the case of other conditions remain unchanged, there was a positive correlation between the RL intensity and the deposited energy.

At the same time, according to the Shockley diode equation, the output current density can be calculated as:

$$J(V) = J_{sc} - J_0\left[\exp\left(\frac{qV}{kT}\right) - 1\right]. \tag{3}$$

And

$$J_{sc} = q\int_{E_g}^{\infty} b_s\,(E,\,T)\,\mathrm{d}E, \tag{4}$$

$$J_0 = q\int_{E_g}^{\infty} \frac{2F_a E^2}{h^3c^2}\exp[(-E)/kT]\,\mathrm{d}E, \tag{5}$$

where J_{sc} and J_0 respectively are the short-circuit current density and the reverse saturation current density, q is the electron charge, V is the voltage, k is the Boltzmann constant, T is the ambient temperature, E_g is the band-gap of the PV materials, b_s (E, T) is the luminescence intensity with photon energy of E, F_a is the environmental geometrical factor which is equal to π, h is the Planck constant, and c is the speed of light. The J_0 depends on the E_g and T in Eq. (5). Analysis of the above formulas was performed to J_0 is a definite value for a given PV materials at room temperature. At the same time, J (V) is affected only by the J_{sc}, and J_{sc} is related to b_s (E, T). This means that the output current density increases with the increased luminescence intensity. The open-circuit voltage V_{oc} can be calculated by using the formula

$$V_{oc} = \frac{kT}{q}\ln\left(\frac{J_{sc}}{J_0} + 1\right). \tag{6}$$

From the analysis, V_{oc} also depends on the J_{sc} for constant k, q, T, and J_0. The maximum output power P_{out} can be given by

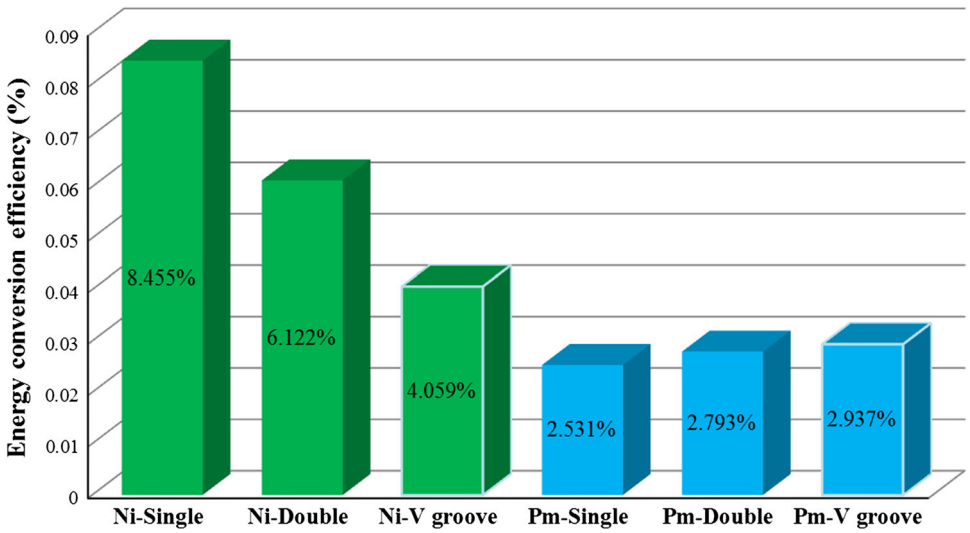

Fig. 11 The energy conversion efficiency of tested phosphor layers

$$P_{\text{out}} = \max\left(J\left(V\right) \times V\right). \tag{7}$$

Since the test conditions are considered as constant, the P_{out} has a significant positive correlation with luminescence intensity.

According to the activity of beta sources given in Table 1, the ideal input power (P_{in}) can be calculated by using the activity A and the average beta energy E_β. In addition, the I–V characteristic curves can be used to evaluate P_{out}. Therefore, we can obtain the energy conversion efficiency (η) as

$$\eta = \frac{P_{\text{out}}}{P_{\text{in}}} = \frac{I_{\text{m}} V_{\text{m}}}{A E_\beta}. \tag{8}$$

Figure 11 gives the energy conversion efficiency of beta RL nuclear battery with different phosphor layer structures. From the reports, the sort order of the experimental conclusions is identical with the simulation results of energy deposition percentage per unit projection area in the phosphor layers. The RL intensity increases with the increase of the deposited energy. For the same test conditions, the electrical performance of the beta RL nuclear battery is related to the RL intensity observed from the ZnS:Cu phosphor layer. Moreover, the phosphor layer structure is one of the most critical factors, which can change the absorbed energy of the incident particles and influence the transmission of the emitted luminescence. Likewise, the coupling of phosphor layer structure with beta source characteristics is a critical factor towards realizing a prospective indirect conversion nuclear battery.

Based on the above analysis, we define the absolute efficiency as:

$$\eta_{\text{abs}} = \eta_\beta \times \eta_{\beta-1} \times \eta_{\text{l-el}} \times \eta_{\text{TR}}, \tag{9}$$

where η_β is the energy conversion efficiency of beta-particle decay energy into useful energy of beta flux coming to the surface, $\eta_{\beta-1}$ is the conversion efficiency of beta particle energy into light energy by a luminescent material, $\eta_{\text{l-el}}$ is the conversion efficiency of the light energy into electrical energy by a PV, η_{TR} is the RL transmission efficiency. η_{TR} is an unknown coefficient which accounts for photon absorption, energy deposited, and other conditions [20]. For given beta source, phosphor layer, and PV devices, the η_{abs} depends on the luminescent transport efficiency η_{TR} under the same irradiation test conditions. According to the above results and analysis, η_{TR} is a tunable parameter and can be substantial improved through using a suitable structure designs to optimize the luminescent transportation. Experimental studies also have proved that a suitable design of phosphor layer structure can availably increase the RL intensity and improve the battery performance. Above all, it can be speculated that elevating the radiation source activity high enough may increase the output power and achieve higher energy conversion efficiency.

Conclusion

It is apparent that the ZnS:Cu phosphor layers can be applied in beta RL nuclear battery as RL materials suitable for energy conversion. The RL spectra and I–V characteristic curves under excitation by the ^{63}Ni and ^{147}Pm beta sources have been utilized to test the batteries with different phosphor layer structure. Their peak emission wavelengths are all at 530 nm. These results show that the RL intensity of the phosphor layers is consistent with the electrical performance under the same test conditions. The structure of the phosphor layers is an important factor having influence on RL intensity and power output. The effects embody in two aspects: absorption of the incident

radiation and transmission of the emitted luminescence. Based on our above-described theoretical and experimental analysis, the tests revealed that (1) the plane phosphor layer with an appropriate thickness can significantly improve the energy conversion efficiency, and (2) the V groove geometry is proved to be an effective method to increasing the power output for a high-energy beta source. In summary, the feasibility of using ZnS:Cu phosphor layers in beta RL nuclear batteries is demonstrated. The results show that the structure design of phosphor layers is a promising path for enhancing the performance of the same type nuclear batteries research.

Acknowledgments Supported by the National Natural Science Foundation of China (Grant No. 11205088), the Aeronautical Science Foundation of China (Grant No. 2012ZB52021), and the Natural Science Foundation of Jiangsu Province (Grant No. BK20141406).

References

1. Saotome Y, Lwazaki H (2001) J Mater Process Technol 119(1):307
2. Liu YP, Tang XB, Xu ZH, Hong L, Wang P, Chen D (2014) Sci China Technol Sci 57(1):14
3. Wang G, Hu R, Wei H, Yang YQ, Xiong XL, Liu GP, Luo SZ (2010) Appl Radiat Isot 68(12):2214
4. Siciliani de Cumis M, Farsi A, Marino F, D'Arrigo G, Marin F, Cataliotti FS, Rimini E (2009) J Appl Phys 106:013108
5. Liu P, Chang YY, Zhang JW (2014) J Micromech Microeng 24(5):055026
6. Prelas MA, Weaver CL, Watermann ML, Lukosi ED, Schott RJ, Wisniewski DA (2014) Prog Nucl Energy 75:117
7. Qiao DY, Chen XJ, Ren Y, Zang B, Yuan WZ (2011) Acta Phys Sin 60(2):155
8. Renschler CL, Gill JT, Walko RJ, Ashley CS, Shepodd TJ, Reed ST, Malone GM, Leonard LE, Ellefson RE, Clough RL (1994) Radiat Phys Chem 44(6):629
9. Sims PE, Dinetta LC, Barnett AM (1994) High efficiency GaP power conversion for Betavoltaic applications. Proceedings of the 13th space photovoltaic research and technology conference 1: 373
10. Sychov M, Kavetsky A, Yakubova G, Walter G, Yousaf S, Lin Q, Chan D, Socarras H, Bower K (2008) Appl Radiat Isot 66(2):173
11. Nath SS, Chakdar D, Gope G, Kakati J, Kalita B, Talukdar A, Avasthi DK (2009) J Appl Phys 105:094305
12. Hong L, Tang XB, Xu ZH, Liu YP, Chen D (2014) Parameter optimization and experiment verification for a beta radioluminescence nuclear battery. J Radioanal Nucl Chem. doi:10.1007/s10967-014-3271-2
13. Wang CF, Li QS, Lu L, Zhang LC, Qi HX, Chen H (2007) Chin Phys Lett 24(3):825
14. Huang JM, Yang Y, Xue SH, Yang B, Liu SY, Shen JC (1997) Appl Phys Lett 70(18):2335
15. Bower KE, Barbanel YA, Shreter YG, Bohnert GW (2002) Polymers, phosphors, and voltaics for radioisotope microbatteries. Florida, Boca Raton
16. Wang GQ, Li H, Lei YS, Zhao WB, Yang YQ, Luo SZ (2014) Nucl Sci Tech 25(2):020403
17. Liu QC, Jia BS, Wan J (1988) Overview of Nuclear Science. Harbin, China
18. Xu ZH, Tang XB, Hong L, Liu YP, Chen D (2014) Nucl Sci Tech 25(4):040603
19. Cress CD, Redino CS, Landi BJ, Raffaelle RP (2008) J Solid State Chem 181(8):2041
20. Schott RJ, Weaver CL, Prelas MA, Oh K, Rothenberger JB, Tompson RV, Wisniewski DA (2013) Nucl Technol 181(2):349